Pseudopotential calculations of nanoscale CdSe quantum dots

Lin-Wang Wang* and Alex Zunger

National Renewable Energy Laboratory, Golden, Colorado 80401

(Received 24 August 1995)

A plane-wave semiempirical pseudopotential method with nonlocal potentials and spin-orbit coupling is used to calculate the electronic structure of surface-passivated wurtzite CdSe quantum dots with up to 1000 atoms. The calculated optical absorption spectrum reproduces the features of the experimental results and the exciton energies agree to within ~ 0.1 eV over a range of dot sizes. The correct form of Coulomb interaction energy with size-dependent dielectric constant is found to be essential for such good agreement.

One of the best-studied quantum dot systems is CdSe.[1–9] It can be prepared[1] with a narrow size distribution of only 5% rms, and was the subject of detailed spectroscopic studies,[1] thus offering the opportunity for detailed comparison between experiment and theory. We will focus here on (i) the dependence of exciton energy E_{ex} on the diameter D of the quantum dot;[1,2,5,6,8] (ii) the changes in optical spectra $\epsilon_2(E)$ with size D.[1,9]

Previous theoretical studies of the spectra of CdSe dots have used the empirically fitted multiband $\mathbf{k} \cdot \mathbf{p}$ method,[3] the tight-binding method,[4,6,9] and the single-band truncated crystal method.[8] We apply here our recently developed mesoscopic-scale pseudopotential method[10–14] to CdSe quantum dots. In this approach we solve via direct diagonalization the single-particle equation for a quantum dot, namely,

$$\left[-\tfrac{1}{2}\nabla^2 + \sum_{n,\alpha} v^{\alpha}(|\mathbf{r} - \mathbf{R}_{n,\alpha}|) \right] \psi_i(\mathbf{r}) = E_i \psi_i(\mathbf{r}), \qquad (1)$$

where $v^{\alpha}(r)$ is the screened pseudopotential of atom of type α at position $\mathbf{R}_{n,\alpha}$. The main features of our approach are as follows.

(i) We use for $v^{\alpha}(r)$ the recently developed[12] nonlocal "semiempirical pseudopotential method" that produces local-density approximation (LDA) quality wave functions with experimentally fit bulk band structures and effective masses. The potentials are nonlocal, contain spin-orbit interactions, and are extracted from LDA calculations on *solids* (not atoms).

(ii) Equation (1) is applied with no further fit to quantum dots. What enables such calculations on ~ 1000 atom systems is the utilization of the "folded spectrum method"[13] (FSM) that provides the exact *near-edge* eigensolutions of Eq. (1) without having to solve for any of the deeper energy levels. The computational effort is thus *linear* with system size.

(iii) Arbitrary shapes of the dot and a realistic surface termination can be explicitly modeled (see below). This is different from surfaceless methods such as $\mathbf{k} \cdot \mathbf{p}$,[3] effective mass,[5] and the truncated-crystal method.[7,8]

(iv) While the FSM provides the discrete near-edge states, our "generalized moment method"[14] (GMM) provides overall information such as density of states (DOS) $n(E)$ and the optical absorption spectra $\epsilon_2(E)$. In this work we neglect electron-electron correlation effects beyond those implicitly present due to fitting the bulk spectra. We obtain $\epsilon_2(E)$ and $n(E)$ over the full valence- and conduction-band energy range, not just near the band edge.[9]

We next discuss some of the details of implementation of the above principles.

(a) *Shapes and structures*: We assume spherical and Se-centered CdSe quantum dots, in the wurtzite crystal structure. We use bulk lattice constants $a = 4.30$ Å, $c = 7.011$ Å. Surface atoms with only one remaining bond have been systematically removed.[15]

(b) *Surface passivation*: In the laboratory made CdSe dots,[1] the surface is capped with organic ligands. To simulate generic passivation we have placed positive (negative) short-range electrostatic potentials ("ligand potential") near the surface Se (Cd) atom. The effective "ligand potentials" are Gaussian $v_0 \exp(-(|\mathbf{r}-\mathbf{R}|/0.79)^2)$ where $|\mathbf{r}-\mathbf{R}|$ is in Å. The origin $\mathbf{R}$ is on the line connecting the missing bonding atom and the passivated atom. The distance between $\mathbf{R}$ and the center of the passivated atom equals αd_0, where d_0 is the bulk Cd-Se bond length. The parameters are determined by fitting to Cd- and Se-terminated flat CdSe surfaces. We find for the Cd atom, $ev_0 = 1.28$ Ry, and $\alpha = 0.55$ (where e is the electron charge), while for the Se atom, $ev_0 = -0.768$ Ry and $\alpha = 0.25, 0.3, 0.4$ for Se atoms with one, two, and three missing bonds, respectively.

We have calculated four CdSe quantum dots: $Cd_{20}Se_{19}$, $Cd_{83}Se_{81}$, $Cd_{232}Se_{235}$, and $Cd_{534}Se_{527}$, with diameters 12.79, 20.64, 29.25, and 38.46 Å, respectively. Our results are shown in Figs 1–4. The densities of states are shown in Fig. 1, where they are compared with the density of states of bulk CdSe. We note from Fig. 1 the following: (i) As the quantum dot becomes smaller, the band gap increases (see Fig. 4 below for more detail). (ii) As the quantum dot becomes smaller, the width W of the upper valence band narrows, as noted by photoemission experiment.[2] We find $W = 3.96, 3.82, 3.62$, and 3.17 eV for our four dots in decreasing size. The bulk value is $W = 4.06$ eV. (iii) In the bulk, there is a density-of-states tail above the conduction-band minimum. In the quantum dot, this tail breaks into a few peaks. For the smallest quantum dot, only one peak is left in that energy region. (iv) There are two new peaks around energy -18 eV. These two peaks represent the surface Se atom s bonding states with one and two missing bonds, respectively.

In Fig. 2, we show the optical absorption spectra [proportional to $\epsilon_2(E)$] of the quantum dots compared with the bulk

results.[16] The predominate feature of quantum dot $\epsilon_2(E)$ is the development of a few strong "excitonic peaks" near the threshold shoulder of the bulk $\epsilon_2(E)$.[17,18] The intensity I of these peaks increases as the quantum dot becomes smaller with a scaling of $I \propto 1/D^3$ for each individual peak. At the same time, the number of peaks is reduced as D decreases. These "exciton peaks" are absent from quantum dots made of indirect-gap materials such as Si.[11] The trend of $\epsilon_2(E)$ as a function of D can be compared with experimental results as reported in Ref. 1. In the experimental data (Fig. 3 of Ref. 1), we indeed see how the smooth absorption shoulder of large, bulklike quantum dots changes into a few peaks, and then how the number of these peaks is reduced and each remaining peak becomes more prominent. This is in agreement with our calculated results.

To compare our calculated $\epsilon_2(E)$ with the experiment more closely, we show in Fig. 3 the calculated $\epsilon_2(E)$ of $Cd_{83}Se_{81}$ ($D=20.6$ Å) and the experimental result of the nearest size $D=23$ Å quantum dots from Fig. 3 of Ref. 1. To make a proper comparison, we have shifted our $\epsilon_2(E)$ downward by 0.65 eV to correct for the Coulomb interaction energy (see below) and for the small difference in dot diameters. The agreement between experiment and theory is very good in that the distances between the two leading peaks are almost the same in the two curves.

Integrating $\epsilon_2(E)$ of Fig. 2, we obtained[11] $\epsilon_\infty^{dot}(D)-1$, i.e., the electronic contribution to the total polarizibility of the quantum dot. To compensate for the fact[12] that the current $\epsilon_2(E)$ is calculated by $|\langle i|\nabla|j\rangle|^2$, instead of $|\langle i|\partial\hat{H}/\partial k|j\rangle|^2$, we have rescaled our integrated result by a factor of 1.178 (which is obtained by comparing the bulk results using these two different transition matrix). We have also added a contribution of 0.63 to the integrated $\epsilon_\infty^{dot}(D)-1$, as we have ignored the d state contributions in our pseudopotential treatment.[12] This contribution is treated as a constant, independent of D since it originated from the deep d states, thus it is affected little by the band change around the band gap. The final bulk result $\epsilon_\infty^{bulk}=6.2$, by the above construction, equals the experimental value. The final $\epsilon_\infty^{dot}(D)$ for dots is plotted as a function of D in Fig. 4(a). These $\epsilon_\infty^{dot}(D)$ data can be fitted as[19]

$$\epsilon_\infty^{dot}(D)=1+(\epsilon_\infty^{bulk}-1)/[1+(7.5\text{Å}/D)^{1.2}]. \quad (2)$$

To calculate the excitonic transition energy $E_{ex}(D)$ from the valence-band maximum (VBM) to conduction-band minimum (CBM) bare band-gap energy $E_g(D) \equiv E_{CBM}(D)-E_{VBM}(D)$ we need to subtract the electron-hole Coulomb interaction energy (in atomic units),

$$E_{ex}(D)=E_g(D)-3.572/D\tilde{\epsilon}^{dot}(D). \quad (3)$$

The last term is calculated via perturbation theory using a $[\sin(2\pi r/D)/(2\pi r/D)]^2$ charge density for both electron and hole and a screening dielectric constant $\tilde{\epsilon}^{dot}(D)$. We first
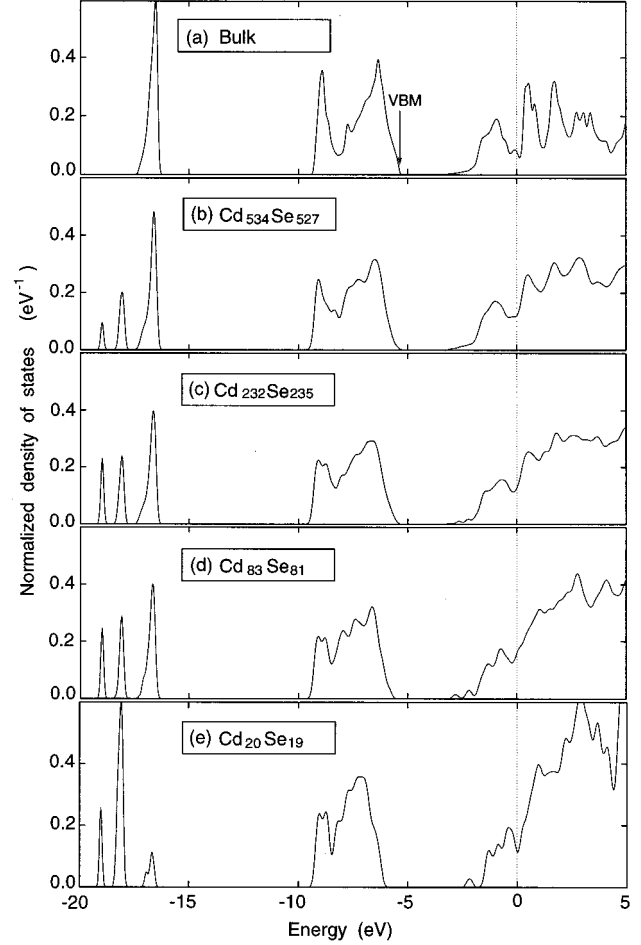
FIG. 1. Density of states for bulk CdSe and for CdSe quantum dots. Results are normalized so that the integral of the valence-band density of states equals 1. The zero is the vacuum level.

discuss $E_g(D)$, then the exciton correction. The CBM state and VBM state wave functions are found to be localized in the interior of the quantum dot, thus the details of the surface structure have only small effects on these states. The energies $E_{CBM}(D)$ and $E_{VBM}(D)$ for our four quantum dots (in decreasing size) are -3.236, -3.091, -2.807, -2.174 and -5.489, -5.617, -5.829, -6.273 eV, respectively. Here the zero is defined as the vacuum level and the bulk E_{CBM} and E_{VBM} values are -5.241 and -3.523 eV, respectively. The energy shifts with D for the VBM and CBM are within 0.1 eV of the tight-binding results of Lippen and Lannoo.[6] The bare (nonexcitonic) band gap $E_g(D)$ is shown in Fig. 4(b) as black dots. It increases by more than 2 eV at the smallest D compared to the bulk value but is still far smaller than the effective-mass results.[1]

The dielectric constant $\tilde{\epsilon}^{dot}(D)$ of Eq. (3) is the screening dielectric constant of the quantum dot, including both the electronic and the ionic contributions for exciton screening. The quantity $\epsilon_\infty^{dot}(D)$ reported in Fig. 4(a) is for total electronic polarization only. One can define another $\tilde{\epsilon}_\infty^{dot}(D)$ explicitly for electronic exciton screening.[11] Because CdSe is not a strong covalent system like Si, we expect smaller $\epsilon_\infty^{dot}(D)$-$\tilde{\epsilon}_\infty^{dot}(D)$ difference than in Si.[11] In this work, we will use $\epsilon_\infty^{dot}(D)$ to approximate $\tilde{\epsilon}_\infty^{dot}(D)$ for the electronic contri-
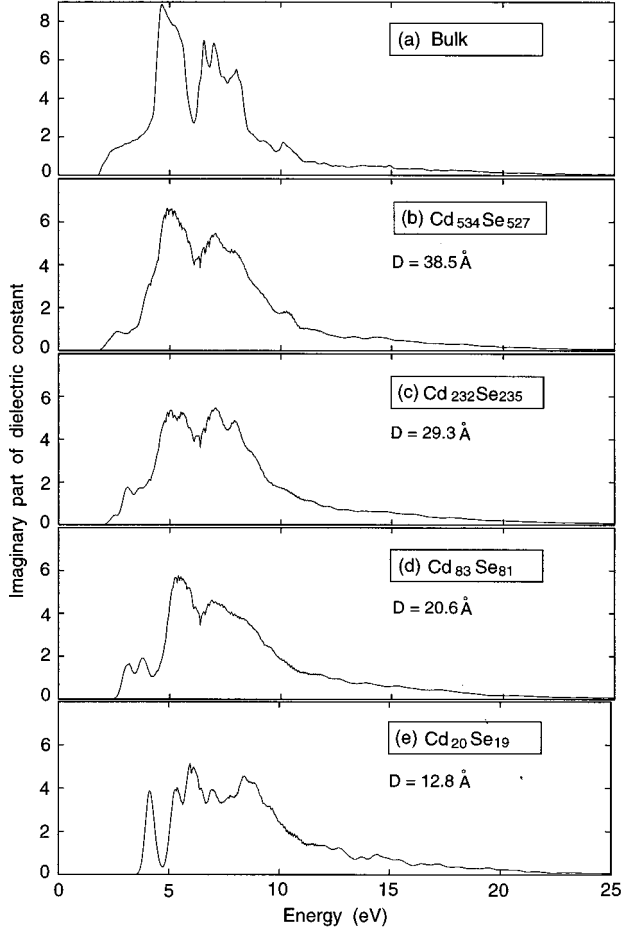
FIG. 2. The imaginary part of the dielectric constant, $\epsilon_2(E)$. They are calculated using the $|\langle i|\nabla|j\rangle|^2$ as the transition matrix and are not rescaled here.
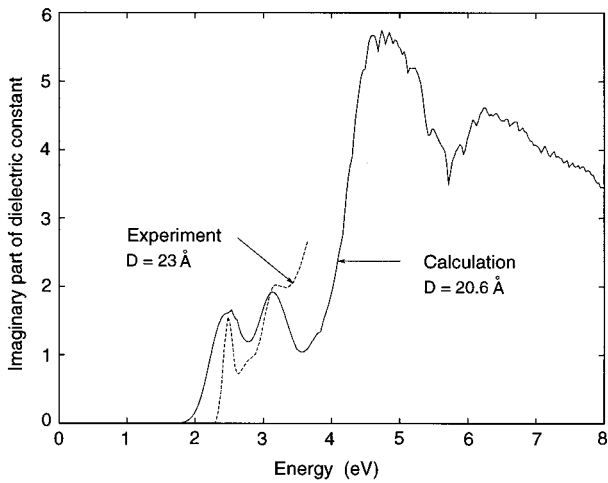
FIG. 3. Comparison between the calculated and experimental absorption spectra. The calculated $\epsilon_2(E)$ has been shifted downward by 0.65 eV to compensate the Coulomb interaction and the small size difference. The experimental data is from Ref. 1.
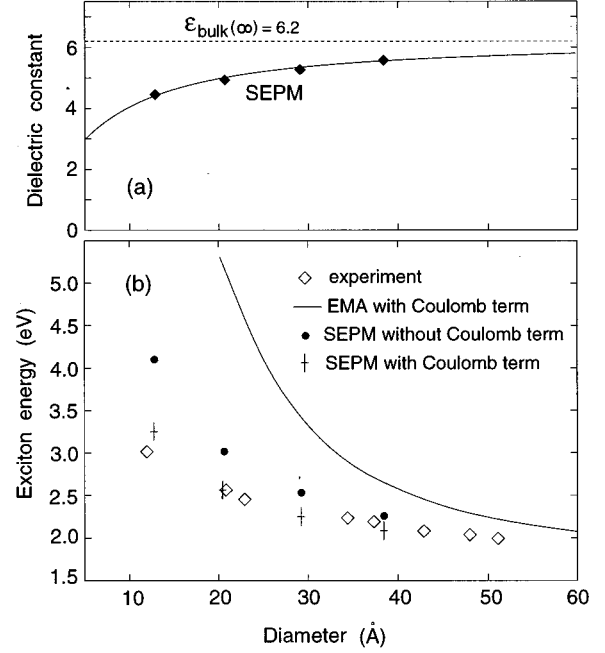
FIG. 4. Quantum dot dielectric constant (a) and exciton energies (b). The solid line in (a) is the fitted result of Eq. (1). The experimental data and the effective-mass (EMA) curve in (b) are both from Ref. 1.

bution to the screening. To include the ionic contribution to the screening, one can define a distance-dependent screening dielectric constant $\epsilon(r_{\text{eh}})$ from

$$V(r_{\text{eh}}) = -1/\epsilon(r_{\text{eh}})r_{\text{eh}}, \quad (4)$$

where r_{eh} is the electron-hole distance and $V(r_{\text{eh}})$ is the screened electron-hole Coulomb potential. Then the expression of $1/\epsilon(r_{\text{eh}})$ derived by Haken[20] for *bulk* exciton screening is

$$\frac{1}{\epsilon^{\text{bulk}}(r)} = \frac{1}{\epsilon_\infty^{\text{bulk}}} - \left[\frac{1}{\epsilon_\infty^{\text{bulk}}} - \frac{1}{\epsilon_0^{\text{bulk}}}\right]\left[1 - \frac{e^{-r/\rho_e} + e^{-r/\rho_h}}{2}\right], \quad (5)$$

where $\rho_e = (2m_e^* \omega_{\text{LO}}\hbar^{-1})^{1/2}$ and $\rho_h = (2m_h^* \omega_{\text{LO}}\hbar^{-1})^{1/2}$. Here, ω_{LO} is the longitudinal-optical–phonon frequency and m_e^* and m_h^* are electron and hole effective masses. For CdSe, $\rho_e \approx 33$ Å and $\rho_h \approx 18$ Å. In Eq. (5) and the following, the subscripts ∞ and 0 stand for $\omega = \infty$ (electronic contribution) and $\omega = 0$ (electronic and ionic contributions), respectively, and $\epsilon_0^{\text{bulk}} = 9.7$. To extend Eq. (5) to the case of the quantum dot, we require that the $\epsilon(r_{\text{eh}}) \equiv \epsilon^{\text{dot}}(r_{\text{eh}}, D)$ in Eq. (4) satisfy $\epsilon^{\text{dot}}(r_{\text{eh}} \to 0, D) = \tilde{\epsilon}_\infty^{\text{dot}}(D)$ and $\epsilon^{\text{dot}}(r_{\text{eh}} \to \infty, D) = \tilde{\epsilon}_\infty^{\text{dot}}(D) + \epsilon_0^{\text{bulk}} - \epsilon_\infty^{\text{bulk}} \equiv \tilde{\epsilon}_\infty^{\text{dot}}(D) + \Delta\epsilon(\text{ion})$. Here we have assumed that the ionic contribution $\Delta\epsilon(\text{ion}) = 3.5$ to the screening is the same for bulk and the quantum dot. Using these requirements for $\epsilon^{\text{dot}}(r, D)$, we can extend Eq. (5) to

$$\frac{1}{\epsilon^{\text{dot}}(r,D)} = \frac{1}{\tilde{\epsilon}_\infty^{\text{dot}}(D)} - \left[\frac{1}{\tilde{\epsilon}_\infty^{\text{dot}}(D)} - \frac{1}{\tilde{\epsilon}_\infty^{\text{dot}}(D) + \Delta\epsilon(\text{ion})} \right]$$
$$\times [1 - (e^{-r/\rho_e} + e^{-r/\rho_h})/2]. \qquad (6)$$

Substituting Eq. (6) into Eq. (4), and using the electron and-hole charge density $[\sin(2\pi r/D)/(2\pi r/D)]^2$, we have numerically calculated the Coulomb interaction energies. To present the result in a simple form, we can retain Eq. (3), with the $\tilde{\epsilon}^{\text{dot}}(D)$ in Eq. (3) expressed as

$$\frac{1}{\tilde{\epsilon}^{\text{dot}}(D)} = \frac{1}{\tilde{\epsilon}_\infty^{\text{dot}}(D)} - \beta(D) \left[\frac{1}{\tilde{\epsilon}_\infty^{\text{dot}}(D)} - \frac{1}{\tilde{\epsilon}_\infty^{\text{dot}}(D) + \Delta\epsilon(\text{ion})} \right].$$
$$(7)$$

The $\beta(D)$'s for the four quantum dots from large to small are 0.348, 0.282, 0.212, and 0.139, respectively. Here $\beta(D)$ indicates how much the ions have participated in the exciton screening. The final calculated exciton energies $E_{\text{ex}}(D)$ using Eqs. (3) and (7) [or, equivalently, from Eqs. (4) and (6)] are shown in Fig. 4(b) as crosses compared with the experimental results (diamonds). Our calculated result agrees very well with the experimental results [the diamonds in Fig. 4(b)] for the range of quantum dot size we have studied. The differences between the calculated and experimental results range from 0.2 eV (the smallest dot) to 0.1 eV (the larger dots). This high degree of agreement demonstrates the quantitative accuracy of the SEPM approach to the electronic

structure calculations of nanostructures. Finally, as shown in Fig. 4(b), the Coulomb interaction energy is large. The use of $\tilde{\epsilon}_\infty^{\text{dot}}(D)$ instead of $\epsilon_\infty^{\text{bulk}}$ is important. However, for the very small quantum dots, the exact formalism of this Coulomb energy via the use of the dielectric constant is far from clear. The ~ 0.2 eV error in Fig. 4(b) for the smallest dot might stem from this uncertainty of the calculated Coulomb energy at that small size range. More work needs to be done to get more accurate results of the exciton energy for this very small size range.

The excellent agreement with experiment for CdSe dots is in contradiction with the situation[10,11,21] for Si dots, where the experiments of Schuppler et al.[22] give consistently lower gaps and weaker size dependence than our calculations, using the same method as that used here. However, the Si data is emission while the CdSe data is absorption. While small basis-set tight-binding models[21] do produce small band gaps for Si dots, in better agreement with emission experiment, our previous calculations (Fig. 4 of Ref. 10) showed that, in part, such lower gaps are an artifact of the small basis. We suspect that the systematically small gaps in Si (Ref. 22) represent a persistent defect level, not intrinsic band-to-band transitions as in CdSe.

---

*Present address: Biosym/MSI, 9685 Scranton Road, San Diego, CA 92121.

[1] C.B. Murray, D.J. Norris, and M.G. Bawendi, J. Am. Chem. Soc. **115**, 8706 (1993).

[2] V.L. Colvin and A.P. Alivisatos, Phys. Rev. Lett. **66**, 2786 (1991).

[3] Al.L. Efros and A.V. Rodina, Phys. Rev. B **47**, 10 005 (1993); A.I. Ekimov et al., J. Opt. Soc. Am. B **10**, 100 (1993); Al.L. Efros, Phys. Rev. B **46**, 7448.

[4] N.A. Hill and K.B. Whaley, J. Chem. Phys. **100**, 2831 (1994).

[5] S. Nomura and T. Kobayashi, Solid State Commun. **78**, 677 (1991).

[6] P.E. Lippens and M. Lannoo, Phys. Rev. B **41**, 6079 (1990); Semicond. Sci. Technol. **6**, A157 (1991).

[7] M.V. Ramakrishna and R.A. Friesner, Phys. Rev. Lett. **67**, 629 (1991); J. Chem. Phys. **95**, 8309 (1991); **96**, 873 (1992).

[8] A. Tomasulo and M.V. Ramakrishna (unpublished).

[9] L.M. Ramaniah and S.V. Nair, Phys. Rev. B **47**, 7132 (1993).

[10] L.W. Wang and A. Zunger, J. Phys. Chem. **98**, 2158 (1994).

[11] L.W. Wang and A. Zunger, Phys. Rev. Lett. **73**, 1039 (1994).

[12] L.W. Wang and A. Zunger, Phys. Rev. B **51**, 17 398 (1995).

[13] L.W. Wang and A. Zunger, J. Chem. Phys. **100**, 2394 (1994).

[14] L.W. Wang, Phys. Rev. B **49**, 10 154 (1994).

[15] In the experiment of Ref. 1, an axial ratio slightly larger than 1 (1.1–1.3) of the quantum dot shape is found. However, for the current purpose of calculating $E_g(D)$ and $\epsilon_2(E)$, its effects should be very small. This is evident from our Si quantum dot calculation (Ref. 10), where we found a unified curve of $E_g(D)$ for different shaped quantum dots provided they are not too prolate.

[16] The small peak (at 2.5 eV) at the shoulder of $\epsilon_2(E)$ in Figs. 9(b) and 9(c) of Ref. 12 is caused by numerical inaccuracy in the $\mathbf{k} \cdot \mathbf{p}$ calculation. Our recent more accurate calculations indicate that that peak should be smoothed away. This does not affect any other results in Ref. 12.

[17] See L.E. Brus, Appl. Phys. A **53**, 465 (1991); M.G. Bawendi, M.L. Steigerwald, and L.E. Brus, Annu. Rev. Phys. Chem. **41**, 477 (1990).

[18] These "excitonic peaks" do not necessarily represent strongly correlated electron-hole pairs. These peaks are actually contributed from electronic excitation with little many-body correlation between the electron and hole, and thus can be described adequately by our single-particle Hamiltonian. This also means that the electron-hole Coulomb interaction can be treated via perturbation theory.

[19] This formula does not have a correct asymptotic form for $D \to \infty$. We only intend to use this formula in a finite-size range, say $D \lesssim 100$ Å.

[20] R.S. Knox, Solid State Phys., Suppl. 5, (1963); H. Haken, Nuovo Cimento **10**, 1230 (1956).

[21] N.A. Hill and K.B. Whaley, Phys. Rev. Lett. **75**, 1130 (1995).

[22] S. Schuppler et al., Phys. Rev. Lett. **72**, 2648 (1994).